

Received 1 May 2023, accepted 28 May 2023, date of publication 31 May 2023, date of current version 7 June 2023.

Digital Object Identifier 10.1109/ACCESS.2023.3281552

RESEARCH ARTICLE

Research on Electric Vehicle Charging Safety Warning Based on A-LSTM Algorithm

XIAOHONG DIAO¹, LINRU JIANG¹, TIAN GAO¹, LIANG ZHANG¹, (Member, IEEE), JUNYU ZHANG², LONGFEI WANG², AND QIZHI WU²

¹Beijing Electric Vehicle Charging Engineering Technology Research Center, China Electric Power Research Institute, Beijing 100192, China

²School of Electrical Engineering, Northeast Electric Power University, Jilin 132012, China

³Key Laboratory of Modern Power System Simulation and Control and Renewable Energy Technology, Ministry of Education, Northeast Electric Power University, Jilin 132012, China

Corresponding author: Liang Zhang (xiaozhanghit@163.com)

This work was supported by the 2022 Beijing Electric Vehicle Charging Engineering Technology Research Center Open Fund Project “Research on Electric Vehicle Adaptive Charging Safety Early Warning Model Based on Deep Learning” under Grant YDB51202101417.

ABSTRACT Accidents involving electric vehicle fires have increased as the number of electric vehicles has grown recently. The issue of charging safety is a key barrier to the growth of the electric vehicle sector because these accidents have resulted in large financial losses for car owners and charging facility operators. The approach for resolving the issue of electric car charging safety through an electric vehicle charging safety warning system is suggested in this research. The suggested solution uses an adaptive optimization of long short-term memory neural network (A-LSTM) to forecast voltage changes throughout the whole charging process by using the vehicle’s daily historical charging data. The warning threshold adjustment method is established by the difference between the predicted voltage data and the actual voltage data, which is dynamically adjusted as the charging process progresses. Finally, a real-time warning model for vehicle charging alert is developed. The daily charging data of electric vehicles is used in the paper to verify the precision of data prediction and the accuracy and timeliness of the model. The study’s findings demonstrate that the early warning model suggested in this paper can quickly send out early warning signals to safeguard the safety of car charging and can identify aberrant charging data.


INDEX TERMS Electric vehicle, charging safety, early warning, A-LSTM algorithm, daily charging data.

I. INTRODUCTION

The ecological and energy crises are becoming increasingly prominent on a global scale. Compared with traditional fuel vehicles, electric vehicles (EVs) have significant advantages in saving oil resources and reducing carbon emissions. They have received attention from governments and automotive companies worldwide, and the number of EVs in use has continued to grow [1], [2]. However, the frequent occurrences of spontaneous combustion and fires in EVs have caused serious economic losses to car owners and charging facility operators, and charging safety issues have hindered the development of EVs and related industries [3], [4]. With the full implementation of the national big data strategy, the trend

of digitalization and intelligence in the automotive industry is becoming more and more obvious. The use of big data research to solve the safety issues of EVs has become an important pathway. The deep integration of EVs and big data will undoubtedly accelerate the transformation of automotive safety regulatory technology, thereby further promoting the high-quality development of China’s EV industry [5], [6].

At present, the research on the safety warning and fault diagnosis of EV charging process has just started. Generally, the traditional research for EV fault diagnosis and warning is done by constructing the electrochemical model of the battery. Seo et al. used a recursive least squares method to detect internal short-circuit faults in batteries based on an equivalent circuit model with the battery open-circuit voltage and state of charge (SOC) as inputs [7]. Zhang et al. electrochemical model of the power battery is constructed, and the battery

The associate editor coordinating the review of this manuscript and approving it for publication was Junho Hong .

status is judged by comparing the charge response information simulated by the battery model and the battery charge status information for charging fault monitoring and early warning [8]. Tran et al. comprehensive consideration of SOC, temperature and state of health (SOH) establishes an equivalent circuit model for lithium-ion batteries, which is capable of estimating the battery state of charge, temperature and health status with high accuracy and can be effectively monitored by the battery management system (BMS) [9]. In addition, some scholars have used the expert system approach for fault detection and early warning. Song designed a comprehensive evaluation index system for charging safety based on expert scoring and other methods from three aspects: power battery, charging equipment and distribution network, and use the gray correlation degree method to determine the weight of each index [10]. Qian et al. designed a safety and protection monitoring device for electric vehicle charging, and then established an early warning model based on the operation status of charging equipment by fuzzy comprehensive evaluation method [11]. EV battery systems are strongly nonlinear and it is difficult to build an accurate model for them. Fearing that a model is usually only applicable to a specific fault type, it requires a lot of modeling work and is inconvenient in engineering.

In recent years, the widespread use of big data and machine learning has also led to new approaches to fault monitoring and early warning. Zhao et al. proposed a fault diagnosis method for electric vehicle battery system based on big data statistical method to construct a more complete battery system fault diagnosis model based on machine learning algorithm and multi-level screening strategy to detect abnormal changes of voltage [12]. Zhang et al. Constructing a charging warning model based on improved grey wolf optimization-back propagation neural network (IGWO-BP) to accurately identify abnormal EV charging voltage conditions for diagnosis and warning [13]. Xia et al proposed a short-circuit fault diagnosis method based on voltage profile correlation coefficients to detect short-circuit faults by capturing the decreasing trend of voltage correlation coefficients of two adjacent cells individually and using recursive sliding windows to maintain the sensitivity of fault detection during operation. [14] Gao et al. constructed an electric vehicle charging process fault warning method based on adaptive deep belief networks, which can accurately warn of faults during the charging process of electric vehicles [15]. Zhang et al. proposed a new method for quantifying electrical safety index system based on comprehensive weights, which is suitable for application to electrical safety protection of electric vehicle charging equipment [16]. Yu combines BP neural networks with outlier testing to achieve charging safety monitoring and fault warning for electric vehicles, and is capable of alerting when charging faults occur in electric vehicles [17]. Yang et al. proposed a current prediction method based on back propagation neural network to estimate the current of cells with external short circuit faults in the battery pack by neural network using only voltage information to achieve

early warning of thermal runaway [18]. The aforementioned methods based on big data and machine learning are able to handle time-series EV charging data, but they are mostly based on laboratory data, and less research has been conducted on daily EV charging data.

In summary, big data research and machine learning algorithms are widely used in the field of fault diagnosis and early warning, however, electric vehicle charging data is time-series data, and the data volume is huge, the input dimension is many, and the coupling is strong, some deep learning algorithms are not well applied in this scene. The time series warning method based on Long Short-Term Memory (LSTM) can predict the future development trend of the data based on current and historical data features, which is suitable for vehicle charging data warning requirements. Therefore, this paper is based on LSTM algorithm to build the vehicle charging safety warning model. Firstly, we analyze and summarize the factors affecting vehicle charging safety by combining the characteristics of vehicle charging data and the charging characteristics of lithium-ion battery, and filter the charging safety warning factors according to the vehicle charging data characteristics by using Pearson correlation analysis to calculate the correlation coefficients between different warning factors; then we construct the A-LSTM prediction algorithm and design the prediction model of charging data, and get the predicted values of electric vehicle charging data by analyzing and learning from the historical data; finally, we combine the A-LSTM prediction algorithm and design the prediction model of charging data. Finally, the dynamic warning threshold method is constructed by combining the predicted value, actual value and charging standard, and the real-time warning model of EV charging safety is designed. Finally, the dynamic warning threshold method is constructed by combining the predicted values, actual values and charging standards to design a real-time warning model for EV charging safety. The daily charging data are analyzed and verified to prove the accuracy and timeliness of the charging safety warning model constructed in the paper.

II. EV CHARGING SAFETY ANALYSIS

A. ANALYSIS OF EV ACCIDENTS

There are significant differences between combustion accidents in new energy vehicles and those in traditional fuel vehicles. Combustion accidents in traditional vehicles are typically caused by non-standard modifications, aging circuits, arson, and other factors, whereas most combustion accidents in new energy vehicles are caused by thermal runaway [19]. The fire scenarios caused by thermal runaway in EVs mainly include five types: lithium-ion battery charging combustion, natural parking combustion, driving combustion, collision combustion, and immersion combustion. According to statistics [20], the accident ratios for these scenarios are shown in Fig. 1, with the highest proportion of combustion accidents occurring when EVs are being charged, parked, or driven. Generally, there are fewer supervisory personnel around vehicles in the charging and parking states

than during driving. Therefore, it is necessary to improve the safety warning system for EV charging and protect the safety of charging EVs.

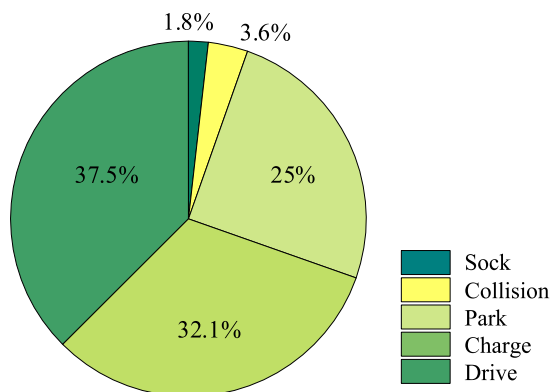


FIGURE 1. EV accident scene diagram.

B. ANALYSIS OF EV CHARGING METHOD

There are two main charging methods used for EVs in the market today, one is Direct Current (DC) fast charging and the other is Alternating Current (AC) slow charging. DC fast charging mainly uses the high-power DC charger of the charging pile to directly charge the EV power battery, which has a higher charging current and requires a short charging time. AC slow charging relies on the on-board charger inside the EV to convert the AC power provided by the charging equipment to DC power for charging the power battery. This charging method has a lower charging current but requires a longer charging time, which generally causes less chemical damage to the battery and can prolong the battery's service life [21], [22]. The voltage and temperature trends of an on-board battery pack change when a vehicle is charged using different charging techniques. Therefore, in order to develop effective charging warning models, it is important to study fast charging and slow charging vehicles separately.

C. ANALYSIS OF THE FACTORS AFFECTING THE SAFETY OF EV CHARGING

Numerous factors are implicated in the safety of EV charging. Typically, mistreatment of the battery can cause a sudden rise in its internal temperature [7], which if exceeds a critical threshold, may result in the melting of the separator, decomposition of the positive electrode material, and electrolyte oxidation within the battery, ultimately leading to a violent combustion event and subsequent thermal runaway. While the phenomena may vary slightly depending on the specific trigger, the underlying mechanisms are largely analogous. In the following, we will provide a comprehensive overview of the commonly observed influential factors.

1) INTERNAL SHORT CIRCUIT IN BATTERY

When a battery is internally short-circuited for some reason, a huge current will be generated inside the battery in a short

period of time, causing the internal temperature of the battery to rise sharply, which will lead to charging accidents. From the perspective of the triggering mechanism, there are three main types of internal short circuits in batteries: internal short circuits caused by overcharge or over discharge, internal short circuits caused by mechanical damage and self-triggered internal short circuits [23].

2) BATTERY OVERCHARGE

Overcharging of a battery can be a dangerous condition where the charging equipment continues to supply energy to the battery for an extended period of time. This can lead to safety accidents. There are several factors that can cause battery overcharging, including high ambient temperatures and incorrect charging methods [24].

3) BATTERY SEPARATOR AND ELECTROLYTE MATERIAL

The battery separator serves the critical function of isolating the positive and negative electrodes to prevent short circuit accidents that may arise from the penetration of the separator during the electrochemical reaction. However, as the battery undergoes cycles of charge and discharge, the electrolyte degrades, leading to a decline in the battery's overall performance over its life cycle [25].

4) BATTERY PACK CONSISTENCY

Due to differences in production technology and daily usage, individual battery parameters of EV battery packs may become inconsistent, and there may be differences between individual batteries due to internal decay effects of the battery pack. The inconsistency of battery packs can lead to differences in SOC, voltage, SOH, etc. between individual cells, which can seriously affect normal use [26].

In summary, it is evident that EV spontaneous combustion accidents are primarily caused by thermal runaway issues resulting from internal battery short circuit, battery overcharge, and battery pack inconsistency. Therefore, this paper integrates vehicle charging data and charging safety influencing factors and selects real-time battery pack SOC, initial SOC, battery pack SOH, charging current, maximum temperature of single battery, and maximum voltage of single battery as EV safety warning factors. Battery pack SOC and charging voltage current temperature can represent the charging status of EV, SOH can represent the aging condition of the battery pack, and the aforementioned early warning factors can be used to determine whether the EV is malfunctioning or not.

III. MODE DESIGN

The safety warning model is developed based on the characteristics of EV charging data, comprising five distinct steps. The first four steps involve offline processing to establish EV charging warning thresholds, while the fifth step involves online comparison of EV charging data with the warning thresholds to achieve status detection and warning. The model operates as follows:

Step 1: EV charging data processing. Firstly, the collected EV historical charging data are subjected to de-hybridization operation to remove missing values and great outliers from the data, and then the data are normalized according to equation (1) to make the EV historical charging data vector \mathbf{EV}_{his} a standard data mapped to $[-1, 1]$. This can prevent the subsequent calculation errors caused by data changes, and at the same time can improve the operation speed and prediction accuracy of the early warning model.

$$\mathbf{EV}_{\text{his-input}} = \frac{2(\mathbf{EV}_{\text{his}} - \mathbf{EV}_{\text{his-min}})}{\mathbf{EV}_{\text{his-max}} - \mathbf{EV}_{\text{his-min}}} - 1 \quad (1)$$

where $\mathbf{EV}_{\text{his-input}}$ is the normalized historical data value, which is used as the standard input data in the subsequent steps; \mathbf{EV}_{his} is the original charging data; $\mathbf{EV}_{\text{his-max}}$ and $\mathbf{EV}_{\text{his-min}}$ are the maximum and minimum values of the corresponding data in the original charging data.

Step 2: EV charging warning factor calculation. First, the EV charging safety warning factor r_{wf} is determined by considering the EV charging history data types and the EV charging safety influencing factors summarized in the introduction section, and then the corresponding data in \mathbf{EV}_{his} , the EV charging history data set, are extracted according to the warning factor, and the correlation coefficient c_k among the influencing factors is calculated by the Pearson correlation coefficient formula shown in equation (2) and equation (3), and finally the correlation coefficients among the factors are compared, and the one with the strongest correlation with other factors is selected as the charging safety warning factor r_{wf} .

$$c_{xy-i} = \frac{\sum_{i=1}^n (x_i - \bar{x})(y_i - \bar{y})}{\sqrt{\sum_{i=1}^n (x_i - \bar{x})^2 \sum_{i=1}^n (y_i - \bar{y})^2}} \quad (2)$$

$$c_k = \sum_{i=1}^m c_{xy-i} \quad (3)$$

where i is the data number of the warning factor, n is the number of input data, x and y are two different warning data. c_{xy-i} shown in Table 1 indicates the correlation coefficient between warning data x and y , \bar{x} and \bar{y} are the average value of the corresponding warning data set, k is the warning factor serial number, m is the number of warning factors, and m is taken as 6 according to Table 1.

Step 3: EV charging data prediction. Extract EV standard charging data $\mathbf{EV}_{\text{his-input}}$ to select suitable parameters as input $\mathbf{EV}_{\text{input}}$, take the predicted data of charging factor as output \mathbf{EV}_{pre} , and build A-LSTM deep network for regression calculation of the data. Observe the prediction results, gradually adjust the hyperparameters of the algorithm, explore the balance between the amount of input data and the prediction accuracy of the algorithm, while ensuring the optimal prediction accuracy and prediction time, determine the optimal hyperparameters of the algorithm, form the A-LSTM deep learning network model, and then use the A-LSTM algorithm to fit the data, as shown in equation (4) and equation (5)

TABLE 1. EV charging safety warning factor.

NO.	Symbols	Meaning of Symbols	Unit
1	$r_{\text{wf-SOC0}}$	Charge initiation SOC	%
2	$r_{\text{wf-SOC}}$	Charging real-time SOC	%
3	$r_{\text{wf-SOH}}$	SOH	%
4	$r_{\text{wf-I}}$	Charging current	A
5	$r_{\text{wf-V}}$	Maximum individual voltage	V
6	$r_{\text{wf-C}}$	Maximum individual temperature	°C

to obtain the EV warning factor prediction vector \mathbf{EV}_{pre} and EV warning factor pressure residual vector \mathbf{EV}_{re} , which lay a good foundation for the subsequent charging warning threshold setting.

$$\mathbf{EV}_{\text{pre}} = f_{\text{A-LSTM}}(\mathbf{EV}_{\text{input}}) \quad (4)$$

$$\mathbf{EV}_{\text{re}} = \mathbf{EV}_{\text{pre}} - \mathbf{EV}_{\text{nor}} \quad (5)$$

Step 4: EV dynamic warning threshold setting. According to the EV prediction data residual \mathbf{EV}_{re} obtained in step 3 and the ‘‘Electric Vehicle Safety Requirements (GB 18384-2020)’’, the vehicle charging voltage threshold array \mathbf{EV}_{thr} is established with the data characteristics. then the vehicle charging process is divided into 4 different warning regions according to the SOC value, I, II, III and IV, considering the changing characteristics of the vehicle charging data, and each region is set up with the warning The threshold adjustment factor w , w is dynamically adjusted according to different regions, and equation (6) constructs the dynamic warning threshold $\mathbf{EV}_{\text{thr-dy}}$ for EV charging warning factor.

$$\mathbf{EV}_{\text{thr-dy}} = \sum_{j=1}^n w_j \mathbf{EV}_{\text{thr-j}} \quad (6)$$

$$\mathbf{EV}_{\text{thr}} = \pm \lambda \cdot \overline{\mathbf{EV}_{\text{re}}} \quad (7)$$

where j is the charging warning region serial number, taking the value of [1] and [4], w_j is the warning threshold adjustment factor of region j , and λ is the adjustment factor, taking the value between $[-1.15, 1.15]$ according to the specific data variation.

Step 5: EV charging safety warning. Input EV real-time charging data \mathbf{EV}_{rt} , record the initial SOC of EV charging as SOC_0 and the highest voltage of vehicle battery as V_0 , determine the vehicle warning area according to the initial state of vehicle charging, then select the dynamic warning threshold of the corresponding area and monitor the vehicle charging status, when the vehicle charging status is abnormal, i.e., the changes of real-time charging voltage, charging current and temperature are different from the safety model constructed based on the historical normal charging data, consider that there is a safety problem of EV charging at this time, implement the corresponding warning rules in time and take measures to deal with it. When the vehicle charging state is abnormal, i.e., the real-time charging voltage, charging current and temperature changes are different from the safety

model built based on the historical normal charging data, it is considered that there is a safety problem in EV charging at this time, and the early warning is carried out in time and measures are taken to deal with it.

The specific EV charging safety warning rules are as follows:

The first level is EV normal charging state, the vehicle charging data in this state is below the warning threshold, which is the most ideal charging state and no alarm will be made;

The second level is EV warning state, the EV SOC in this state is below 60% and the maximum battery voltage is higher than the warning threshold, the state of this level indicates that the EV charging is abnormal and protective measures should be taken in time to make it converge to normal charging;

The third level for the electric vehicle alert state, the state of the vehicle SOC in 60%-80%, the vehicle single battery maximum voltage is higher than the warning threshold, at this time the vehicle state may have risk, should be alarmed and timely measures to prevent the vehicle from danger;

The fourth level is EV dangerous state, the state of the vehicle SOC is above 80%, the highest voltage of the vehicle single battery is higher than the warning threshold and lasts for a long time, the EV continues to charge in this state is very likely to burn the car accident, should promptly cut off the power and stop charging.

In summary, the EV charging safety warning model is constructed, and the specific model operation block diagram is shown in Figure 2.

has proven effective in analyzing and learning input vehicle historical charging time series data and forecasting the trend of subsequent charging data based on the historical and current state. Therefore, this study adopts LSTM to address the data regression prediction challenge and further optimizes the problem solution by constructing an A-LSTM model.

A. LSTM ALGORITHM

The LSTM neural network is a variant of Recurrent Neural Network (RNN) that addresses the problems of gradient vanishing and explosion. It replaces the hidden layer of the original RNN with LSTM units, which contain input, output, and forget gates. The forget gate regulates the amount of historical input by controlling which information is retained and which is discarded. The activation function of all three gates is the sigmoid function, which produces values between 0 and 1. The gates learn to weight the historical input, current input, and historical output, thereby achieving the memory function of historical input and output.

The LSTM unit is constructed as shown in (8) to (13), with the candidate LSTM memory cell state value represented by:

$$\tilde{C}(t) = \tanh(\omega_x x(t) - c_x(t) + \omega_{hc}h(t-1) + b_c) \quad (8)$$

where: $x(t)$ is the input data of the historical charging of the EV at the current moment, $h(t-1)$ is the output of the LSTM unit at the previous moment, ω_x and ω_{hc} are the connection weights corresponding to the two inputs $x(t)$ and the output $h(t-1)$, $\tilde{C}(t)$ is the memory unit reference, and b_c is the bias of the network. Values of the input gates of the LSTM network:

$$I(t) = \text{sigmoid}\left(\begin{matrix} \omega_{xi}x(t) + \omega_{hi}h(t-1) \\ + \omega_{ci}C(t-1) + b_i \end{matrix}\right) \quad (9)$$

where: ω_{xi} , ω_{hi} and ω_{ci} are the input data for the current moment of EV historical charging, the previous moment LSTM cell output and the previous moment cell output connection weights to the input gate, respectively, and b_i is the bias of the input gate.

The values of the forgotten gates of the LSTM network:

$$F(t) = \text{sigmoid}\left(\begin{matrix} \omega_{xf}x(t) + \omega_{hf}h(t-1) \\ + \omega_{fi}C(t-1) + b_f \end{matrix}\right) \quad (10)$$

where: ω_{xf} , ω_{hf} and ω_{fi} are the EV historical charging input data at that moment, the previous moment LSTM cell output and the previous moment cell output connection weights to the forgetting gate, respectively; b_f is the bias of the forgetting gate.

In this way, the current LSTM memory cell state value:

$$C(t) = F(t) \otimes C(t-1) + I(t) \otimes \tilde{C}(t) \quad (11)$$

where \otimes denotes the residence product operation.

And the value of the output gate of the LSTM network:

$$O(t) = \text{sigmoid}\left(\begin{matrix} \omega_{xo}x(t) + \omega_{ho}h(t-1) \\ + \omega_{co}C(t-1) + b_o \end{matrix}\right) \quad (12)$$

where: ω_{xo} , ω_{ho} and ω_{co} are the connection weights of the current moment's input, the previous moment's LSTM cell

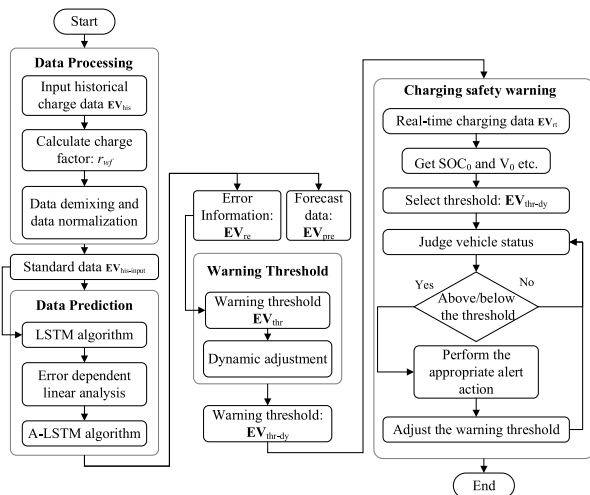


FIGURE 2. Flow chart of EV charging safety warning model.

IV. EV CHARGING DATA PREDICTION MODEL

The third step of the charging safety warning model constructed in Section III, accurate prediction of the complete change pattern of EV charging data is crucial. It is apparent that EV charging data series represent standard time series data, and predicting the variable constitutes a regression problem for time series analysis. LSTM algorithm model

output and the previous moment’s cell output to the output gate, respectively, and b_o is the bias of the output gate.

It is feasible to determine the output of the LSTM memory cell at a given time t by combining equations (8) to (13).

$$h(t) = O(t - 1) \otimes \tanh(C(t - 1)) \quad (13)$$

In summary, the working process of LSTM can be simplified as follows: given the input value $x(t)$ at the current time step, the information is filtered through candidate memory cells, under the control of the input gate, to update the current memory cell. The forgetting gate determines whether the current memory cell can access information from the previous cell, and the valuable information retained by these two parts (i.e., the updated memory) is passed to the next LSTM. The output gate controls whether the information in the memory cell is transmitted to the hidden state for use in the output layer, and $h(t)$ is also connected to the next LSTM cell module. The interaction and control of the three gates allows for the longer-term memory of the input information.

B. A-LSTM ALGORITHM

To enhance the precision of the LSTM model’s predictions and mitigate its error, this study utilizes the error correlation linear analysis approach and proposes the A-LSTM (Adaptation LSTM) model. This model involves developing a relationship equation (13) that correlates the input variables with the historical prediction error.

$$e_h = f(x_1, \dots, x_n) \quad (14)$$

where: e_h represents the LSTM historical prediction error; $f(x_1, \dots, x_n)$ is a primary function on the input, (x_1, \dots, x_n denotes the input).

The prediction model after error correction is shown in equation (14).

$$h_{A-LSTM} = f(x_1, \dots, x_n) + h(x_1, \dots, x_n) \quad (15)$$

where: $h(x_1, \dots, x_n)$ is the established LSTM prediction model; $f(x_1, \dots, x_n)$ is the error linear correction function, and h_{A-LSTM} is the final output of the A-LSTM algorithm.

V. EXPERIMENTAL VERIFICATION AND ANALYSIS

To validate the proposed EV warning model, this paper selected two types of daily charging data from vehicles for charging characteristic analysis and experimental simulation verification. The charging data of vehicles using fast charging and slow charging were collected separately. The selected vehicles in this study have a demonstrative effect and can serve as a reference for developing other EV charging safety warning models.

A. EV CHARGING DATA

The EV battery system used in this study consists of 18650 type ternary lithium-ion batteries. The EV is composed of 92 individual cells connected in series to form one group, and a total of 32 groups are connected in parallel to form

the battery pack of the EV. Each individual cell has a rated voltage of 3.7V and a rated capacity of 2.2Ah. Therefore, the rated voltage and capacity of the EV battery pack are 328.5V and 69Ah, respectively. Throughout the entire charging process, the EV adopts a typical three-stage charging method, with slow charging before the battery pack’s SOC reaches 80% using constant current charging. The charging termination voltage of the vehicle’s battery system is 377V, and the discharge termination voltage is 276V. The operating temperature range for charging is between 0 to 50°C, and for discharging, it is between -20 to 60°C. The maximum continuous charging current allowed is 35A, and the maximum continuous discharge current is 103A. The charging protection voltage for each individual cell is 4.1V, and the discharge protection voltage is 3V.

The experimental EV operating data is presented in Table 2, which includes fundamental information on vehicle operation and data related to the vehicle battery system.

TABLE 2. Summary of EV Charging Data.

Type	Name	Data Range	Unit
EV operation information	Data Submission Time	—	—
	Motor temperature	-10~50	°C
	SOC	0~100	%
EV battery pack related information	SOH	94.0~96.5	%
	EV charging status	0, 1, 2	—
	Charging current	1~110	A
	Battery temperature	-10~50	°C
	Maximum (low) voltage of single battery cell	3.61~4.15	V

B. EV CHARGING DATA PRE-PROCESSING

In this study, a total of 153,247 vehicle charging history data are collected, with a data time span of 1 year, specifically containing the basic data of vehicle-pile communication and the data type required for the model, which can depict the vehicle charging scenario more completely. External factors, such as measurement errors of vehicle sensors and transmission errors of data, may lead to null values, abnormally large values, and repeated values in historical charging data. Moreover, due to the high data collection frequency, multiple charging data correspond to the same SOC value when the vehicle SOC accuracy is kept to 1 decimal place. Therefore, data de-aggregation is required. After screening and eliminating the abnormal data and blank data, the remaining valid charging data are 98581. Then, the data were normalized to meet the input requirements of the model prediction algorithm.

After data pre-processing, extract the relevant charging data, and equations (2) and (3) were used to calculate the

correlation coefficients c between the real-time SOC of the battery pack, the initial SOC of the battery pack charging, the SOH of the battery pack, the charging current of the battery pack, the maximum temperature of the single cell, and the maximum voltage of the single cell. The purpose was to investigate the degree of coupling between these factors and to determine the charging safety influence factor r_{wf} . The results of these calculations are presented in Fig. 3.

The strength of the correlation between two variables is indicated by the absolute value of the Pearson correlation coefficient, with a value closer to 1 indicating a stronger correlation. Fig. 3, which displays the correlation coefficient heatmap, indicates that the real-time SOC of the battery pack is strongly correlated with both the EV charging current and the highest single cell voltage of the battery pack. The health of the battery pack is strongly correlated with the initial SOC of the battery pack charging. In contrast to the exposition of related literature, the maximum temperature of the single cell of the battery pack is weakly correlated with other factors. Upon ranking, it was discovered that the maximum temperature of the single cell of the battery pack is more significantly impacted by the ambient temperature, and that it changes more under different ambient temperature conditions.

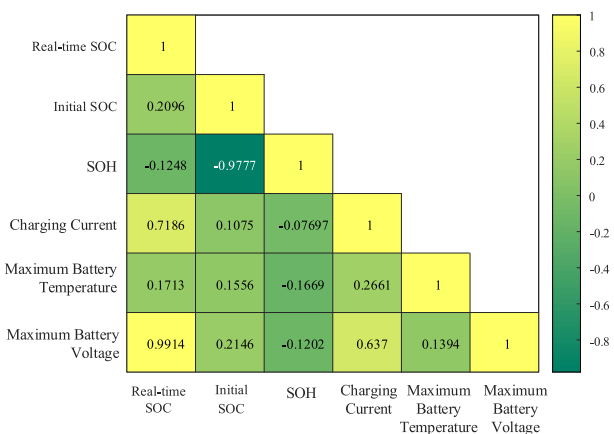


FIGURE 3. Pearson coefficient between parameters.

In order to consider the influence of ambient temperature, this paper selects the vehicle temperature in winter and summer when the ambient temperature difference is large to study, and integrates the EV motor temperature and battery temperature change as shown in Fig. 4. As evident from the figure, the difference between temperature values in January and August is significant, regardless of whether it is the battery or motor temperature. This is also why temperature has a weak correlation with other factors. The motor temperature curve demonstrates that it changes less and stabilizes gradually after a period of charging, while the battery temperature changes continuously during charging. Hence, this paper uses the stable motor temperature as the reference for the ambient temperature and reconstructs the battery temperature by calculating the difference between

the stable motor temperature and the battery temperature. The correlation coefficient of each parameter was then recalculated, as presented in Figure 5. Upon comparing Figure 3 and Figure 5, it is observed that the correlation coefficients between temperature (after the improved formulation) and other factors, except SOH, are significantly improved. This is due to the narrow SOH range (94% to 96.5%) of the EV data obtained in this study, which is not enough to cover the entire SOH cycle.

Upon comprehensive observation of the correlation coefficients between the factors compared in Fig. 5, it is evident that the correlation between single cell voltage and the other factors is stronger when considered together. Therefore, single cell voltage is selected as the warning factor.

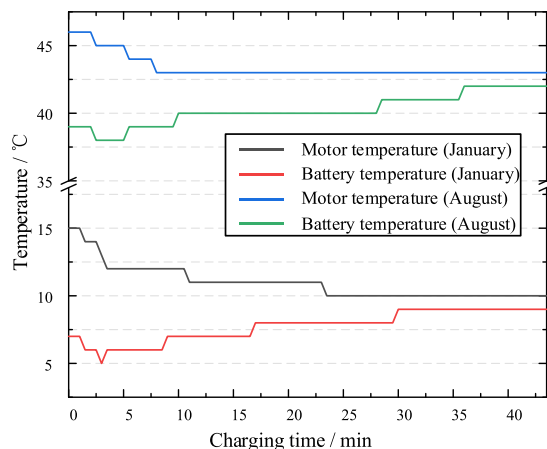


FIGURE 4. Charging temperature curve of vehicle motor and battery in January and August.

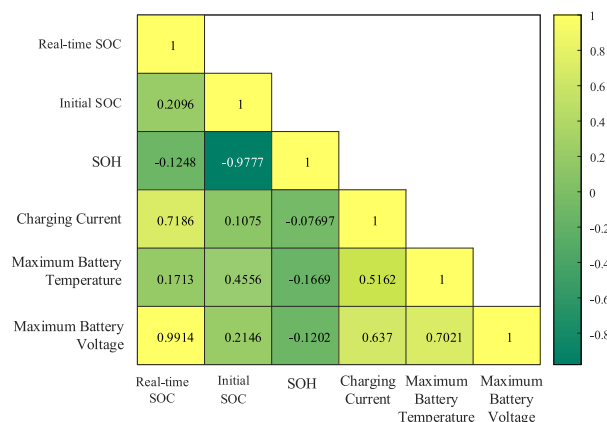


FIGURE 5. Pearson coefficient after improved temperature expression.

C. CHARGING VOLTAGE PREDICTION

To construct a sound algorithm model, it is crucial to determine the primary hyperparameters of the A-LSTM algorithm, which includes the number of neural units in the input and output layers, the number of layers in the hidden layer, and the number of neural units in the hidden layer. Additionally, we have selected the root mean square error δ_{RMSE}

TABLE 3. Results of MAE with different parameters of A-LSTM.

		Number of implied layers			
		1	2	3	4
Number of neurons	50	0.016306	0.014884	0.0097496	0.0094464
	100	0.0087073	0.0085165	0.007558	0.0077584
	150	0.0092994	0.0086817	0.0079107	0.0092439
	200	0.014884	0.0090652	0.008208	0.0068189

TABLE 4. A-LSTM RMSE results with different parameters.

		Number of implied layers			
		1	2	3	4
Number of neurons	50	0.012099	0.0098941	0.0071593	0.0068011
	100	0.0066321	0.0063512	0.0052183	0.0053847
	150	0.0070102	0.0058953	0.0054527	0.0065878
	200	0.0098941	0.0067912	0.0054627	0.0093

(Root Mean Square Error, RMSE) and mean absolute percentage error s_{MAE} (Mean Absolute Error, MAE) as the evaluation criteria to assess the prediction performance of the A-LSTM algorithm under different parameters. The specific formulas for these two evaluation criteria are shown in (16) and (17).

$$s_{RMSE} = \sqrt{\frac{\sum_{i=1}^n (y_i - f_i)^2}{n}} \tag{16}$$

$$s_{MAE} = \frac{1}{n} \sum_{i=1}^n |y_i - f_i| \tag{17}$$

where: f_i is the predicted value of the data, y_i is the original value of the data, and i is the ordinal number of the data ($i = 1, 2, \dots, n$).

The input for the A-LSTM algorithm consists of the initial SOC, real-time SOC, battery pack SOH, charging current, and temperature during EV charging, resulting in an input dimension of 5. The maximum voltage of single cell during charging is selected as the output, resulting in an output dimension of 1.

To identify the optimal parameters, the number of implied layers of A-LSTM is selected as 1-4 layers in turn, and the number of neurons per layer of implied layers is 50, 100, 150, 200 to find the optimal parameters. The prediction results and evaluation indexes are computed for each set of parameters. The output results of the two evaluation indexes are presented in Table 3 and Table 4.

The results presented in Tables 3 and 4 indicate that the optimal evaluation metrics for the A-LSTM model were achieved when the number of hidden layers was set to three and each layer contained 100 hidden units. Based on this finding, the structure of the A-LSTM model was finalized

to include three hidden layers, with each layer containing 100 units. The remaining hyperparameters of the A-LSTM model are provided in Table 5.

TABLE 5. Hyperparameter setting of A-LSTM model.

Hyperparameters	Values
Max Epochs	2000
Mini Batch Size	128
Learn Rate Drop Period	150
dropout	0.4
Learn Rate Drop Factor	0.4

Once the parameters of the A-LSTM model were determined, the algorithm was utilized to fit the historical charging voltages of the vehicle. A subset of the prediction results obtained from the test set are presented in Fig. 6, and Fig. 7 illustrates the absolute error between the predicted and actual values of the selected dataset.

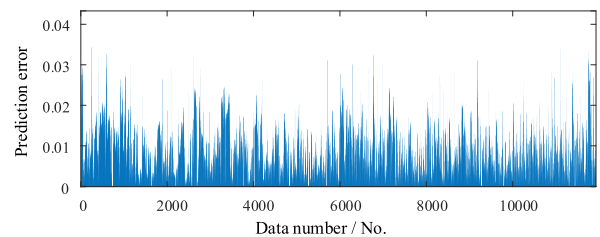


FIGURE 6. EV charging data prediction error.

From Figures 6 and 7, it is evident that the proposed algorithm yields high accuracy in prediction the maximum voltage of the individual battery during the charging of EVs.

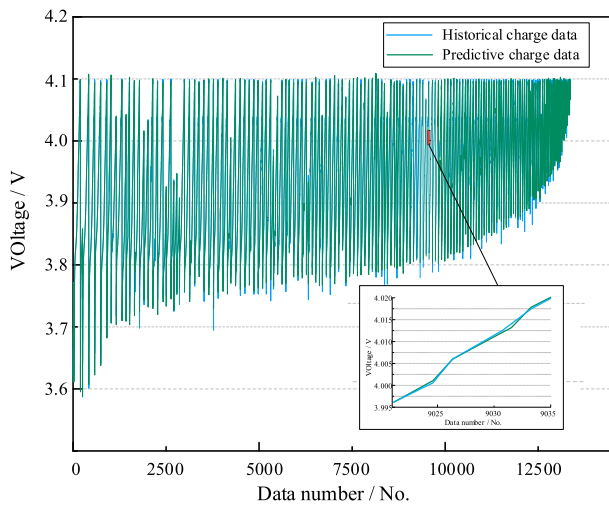


FIGURE 7. Comparison of prediction results.

This facilitates the prediction of the entire voltage change process during vehicle charging. The variation in initial SOC from 0 to 99.9% during charging is illustrated in Fig. 8. The results obtained from the A-LSTM algorithm developed in this study demonstrate excellent prediction performance, completely covering the state of charge for each type of charging, thereby highlighting the exceptional predictive accuracy of the proposed prediction algorithm.

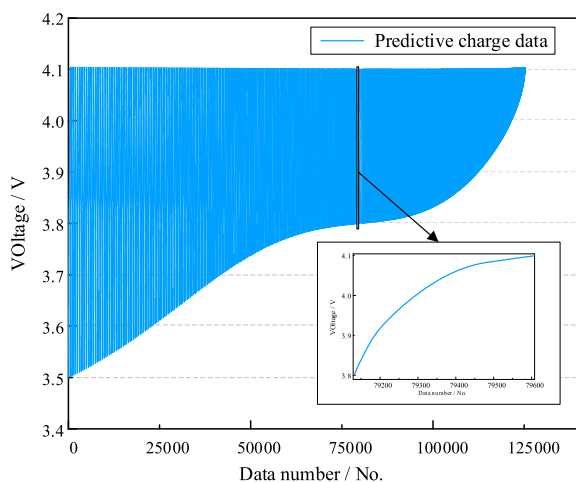


FIGURE 8. EV charging data forecast results.

To verify the prediction accuracy of the A-LSTM model proposed in this paper, we selected BP neural network, RNN neural network, LSTM neural network, and A-LSTM neural network to fit the charging voltage of the vehicle. The BP neural network was set up with 3 fully connected layers, while the RNN, LSTM, and A-LSTM neural networks were set up with 3 layers, and the number of hidden units in each layer was set to 100, respectively. We compared the prediction results of these algorithms using the coefficient of

determination (R^2), as shown in equation (18). The specific prediction results are shown in Fig. 9.

$$R^2 = 1 - \frac{\sum_i (f_i - y_i)^2}{\sum_i \left(y_i - \frac{1}{n} \sum_{i=1}^n y_i \right)^2} \quad (18)$$

where f_i is the predicted value of the data, y_i is the original value of the data, and i is the ordinal number of the data ($i = 1, 2, \dots, n$).

As depicted in Figure 9, it can be observed that for the EV data in the test set, the A-LSTM algorithm prediction results are evenly distributed in the center of the graph, with a maximum R^2 value of 0.99781. This indicates that the algorithm can more accurately predict voltage changes during EV charging, providing reliable prediction data and residual data for the subsequent charging warning threshold setting.

To further compare the performance of LSTM and A-LSTM algorithms, we calculated the prediction residuals using the EV test set data. The distribution histogram was plotted as shown in Figure 10. It is observed that the residuals of the A-LSTM algorithm are primarily distributed in the range of -0.01238 to 0.006933 , whereas the prediction residuals of the LSTM algorithm are distributed in the range of -0.01619 to 0.009573 . This indicates that the A-LSTM algorithm exhibits higher prediction accuracy than the LSTM algorithm.

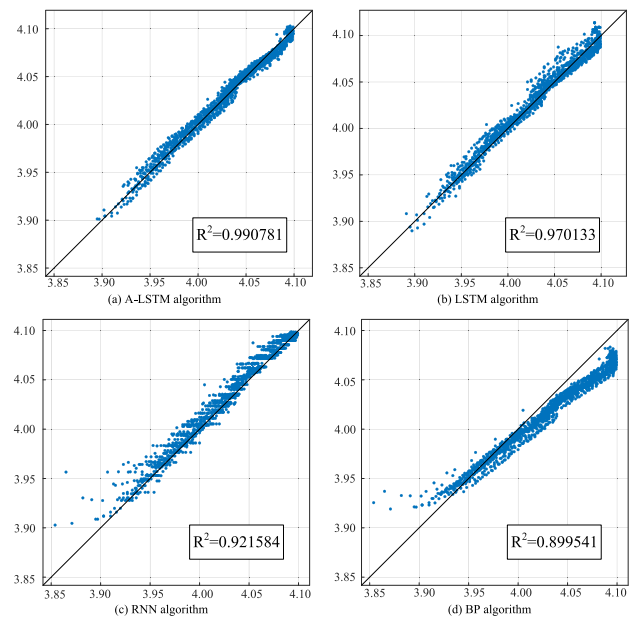


FIGURE 9. Comparison of R^2 values tested by different algorithms.

D. EV CHARGING SAFETY WARNING EFFECT

To establish the vehicle warning threshold, we utilized the dynamic threshold model after obtaining the vehicle charging prediction value. Specifically, we selected a charging dataset and constructed the warning threshold based on the dynamic

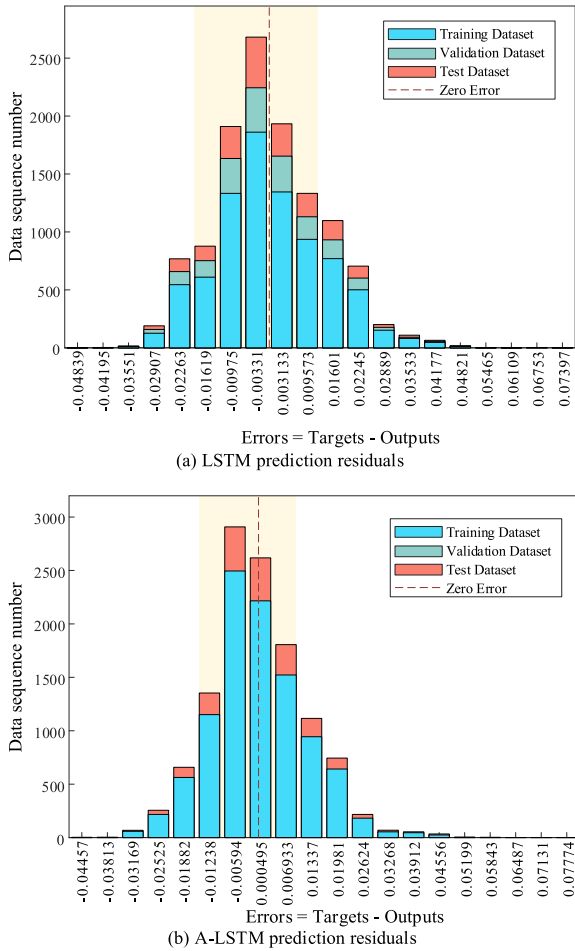


FIGURE 10. Histogram of prediction residuals for different algorithms.

threshold construction rules illustrated in Figure 11. This construction approach divided the charging curve into four regions based on voltage change characteristics.

In warning area I, where the SOC is between 10% and 30%, the voltage rises rapidly while remaining at a low level. To accommodate this situation, we set the warning threshold to $\pm(1.12\% \sim 1.16\%)$ of the normal value. As in warning area II (SOC 30%~60%), the voltage gradually rises, and its increase slows down. we set the warning threshold to $\pm(1.08\% \sim 1.12\%)$ of the normal value. Consequently, the warning threshold is smaller than the previous area. And in warning area III (SOC 60%~80%), the voltage is high, but its increase slows down even further, resulting in an increased risk of overcharging. Here, we set the threshold to $\pm(1.05\% \sim 1.08\%)$ of the normal value. Finally, in Region IV (SOC 80%~100%), the battery is near completion, and the voltage is about to reach its peak, making it susceptible to overcharging, we set the threshold to $\pm(1.03\% \sim 1.05\%)$ of the normal value. If any abnormality is detected in the battery, the warning threshold range will be further contracted.

Figure 12 illustrates how we adjusted the warning threshold after detecting abnormal data in warning area III.

As shown, the warning threshold of voltage changes over time and gradually shrinks with an increase in SOC range. Compared to a fixed threshold, a dynamic threshold is more flexible in warning vehicles during charging while ensuring safety, thereby maximizing the safety of the vehicle charging point.

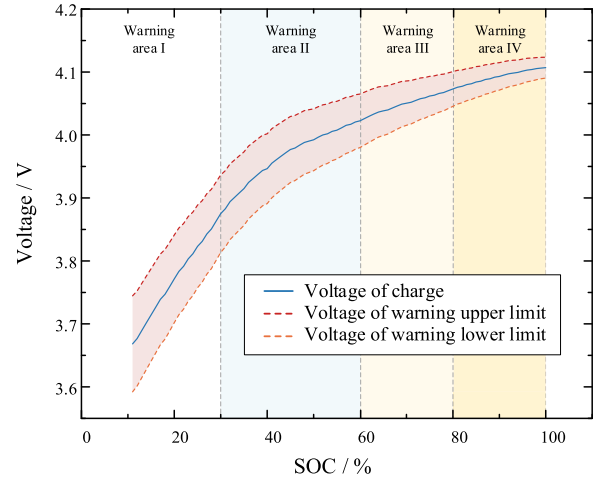


FIGURE 11. Dynamic warning threshold.

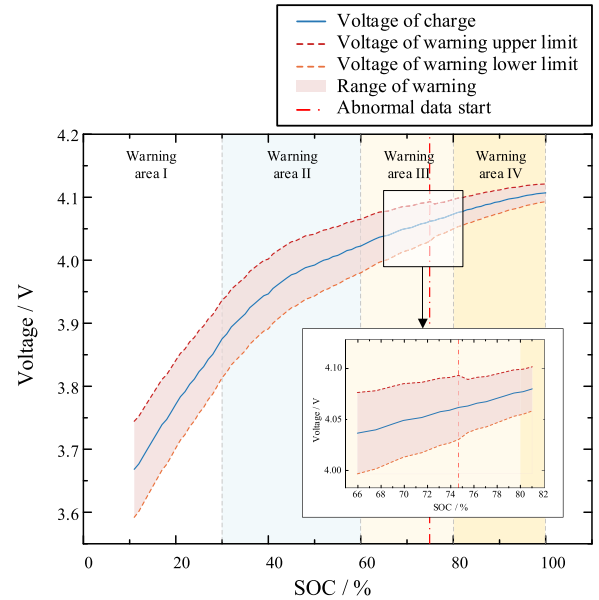


FIGURE 12. Dynamic warning threshold after adjustment.

As the collected EV charging data did not include any fault data, we simulated three types of vehicle fault state data to assess the accuracy of the early warning model. To generate this data, we used the fault data setting method outlined in Table 6. And then we calculated the accuracy of the model using equation (19).

$$w_a = (N_{det}/N_{err}) * 100 \tag{19}$$

$$V_{err} \in (\text{rand}(-0.1 \sim 0.1) * V_{nor}) \tag{20}$$

TABLE 6. Simulated vehicle failure data.

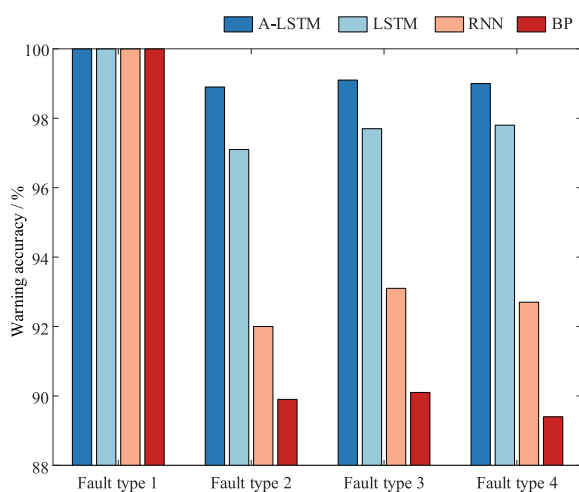
Fault type	Data description
Data transmission failure	Randomly insert 100 sets of empty data and wrong data in the data set
Discrete data faults	Randomly insert 200 sets of discrete abnormal voltage data in the data set according to (20)
Continuous data failure	Insert 200 sets of continuous abnormal voltage data randomly in the data set according to (21) Insert 200 sets of random anomalies when the SOC is above 75 according to (22)
Critical charge failure	

$$V_{err} \in (\text{rand}(-0.15 \sim 0.15) * V_{nor}) \quad (21)$$

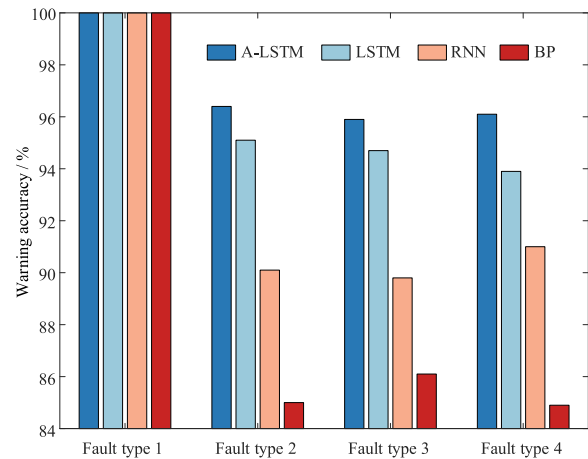
$$V_{err} \in (\text{rand}(-0.25 \sim 0.25) * V_{nor}) \quad (22)$$

where w_a is the warning accuracy, N_{det} is the number of fault data detected by the model, and N_{err} is the number of fault data set in this paper, V_{err} represents the fault voltage data set, V_{nor} represents the normal charging data, and 'rand()' represents a function that generates a random number.

To validate the accuracy of the proposed charging warning model, we used the predicted data from the BP neural network, RNN neural network, LSTM neural network, and A-LSTM neural network (as discussed in section IV-A) to construct fixed warning thresholds and dynamic warning thresholds. We then ran the warning models in a sequence and recorded the warning accuracy. The results of our analysis are presented in Fig. 13 and Fig. 14.

**FIGURE 13. Dynamic threshold warning accuracy rate.**

According to Fig. 13, for fault type 1, all four prediction algorithms can accurately identify empty data and abnormal data thanks to the proposed warning architecture in this paper.

**FIGURE 14. Fixed threshold warning accuracy.**

For fault types 2, 3, and 4, the proposed warning model in this paper can accurately indicate the charging faults of vehicles, with an average accuracy rate of 99.0%. By comparing Fig. 13 with Fig. 14, it can be concluded that the dynamic warning thresholds proposed in this paper can improve the accuracy of charging safety warnings for all four types of faults. For fault types 2 and 4, the dynamic threshold can improve the warning accuracy rate by an average of 2.51%. Particularly for the third charging fault type, the dynamic threshold can improve the average warning accuracy rate by 5.84% compared to using a fixed threshold. This is because the warning model constructed in this paper can accurately and strictly monitor and warn the subsequent charging process by dynamically reducing the warning threshold after the fault is identified.

Another element in evaluating the warning model is the warning time. In this study, the ΔSOC , as shown in equation (23), is chosen as the measure of the vehicle warning time, where a lower ΔSOC value indicates better warning results.

$$\Delta\text{SOC} = \text{SOC}_{err} - \text{SOC}_{det} \quad (23)$$

where SOC_{err} represents the SOC at the beginning of the fault, while SOC_{det} represents the SOC at which the fault was detected. A smaller value of ΔSOC indicates that the model can detect vehicle faults in a timely manner.

Then we set the abnormal voltage value using equation (18), and identified the corresponding SOC interval in which the voltage was located as shown in Table 5. Next, we executed the warning model sequentially for each SOC interval in Table 5, and the results are presented in Fig. 15.

As shown in Fig. 15, the dynamic threshold warning model proposed in this paper can provide early warning for faults in a short period of time. For the first type of fault, since the SOC is low at this time and in order to prevent false alarms, the dynamic threshold is set relatively loose. Therefore, the required warning ΔSOC is 3.8%. For fault type 3, the SOC and battery voltage are both in a relatively high state. To ensure the safety of the vehicle to the greatest extent

possible, the warning threshold is set more strictly, with a required warning Δ SOC of 0.8%. Compared with the fixed threshold, the dynamic threshold proposed in this paper for charging safety warning has excellent warning timeliness.

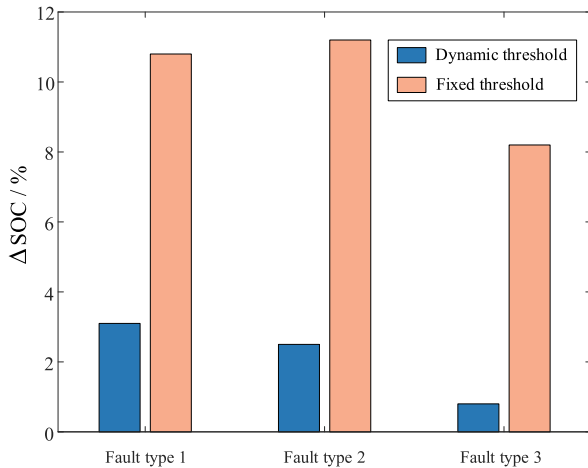


FIGURE 15. Time-limit of warning for different models.

VI. DISCUSSION

The following conclusions can be drawn from the analysis of the results over time:

- 1) The actual charging data of EVs obtained has abnormal samples due to sensor failures and transmission problems. Eliminating data anomalies through data preprocessing can improve the prediction accuracy of the algorithm;
- 2) EV battery temperature is greatly influenced by the external environment, by smoothing the motor temperature and battery temperature at the same time, the environmental influence can be significantly reduced, providing convenience for subsequent data prediction;
- 3) A-LSTM algorithm for time series data prediction problems: the accuracy and applicability of A-LSTM for EV voltage prediction problems is demonstrated by comparison with three other algorithms;
- 4) The construction of dynamic thresholds can significantly improve the prediction accuracy and timeliness of the model. Comparing dynamic thresholds with fixed thresholds, it was found that the dynamic thresholds had an average 4.52% higher accuracy in predicting charging anomalies for different vehicles and the required Δ SOC for warning was reduced by an average of 8.21%.

VII. CONCLUSION

This paper proposes a state monitoring and fault warning method for electric vehicle charging processes based on charging-side deep learning. The aim of the method is to ensure the safety of electric vehicle charging, promote the integration of automotive safety technology with various data

resources, and facilitate the implementation of the national big data strategy.

The proposed method can effectively monitor various physical quantity data of EV charging, enable charging fault warning of EV, and prevent false alarms caused by incorrect charging data. However, this study has some limitations, particularly in terms of data acquisition of SOH and the lack of complete life cycle EV charging data. Further research could explore these areas in greater depth.

REFERENCES

- [1] X. Feng, Y. Pan, X. He, L. Wang, and M. Ouyang, "Detecting the internal short circuit in large-format lithium-ion battery using model-based fault-diagnosis algorithm," *J. Energy Storage*, vol. 18, pp. 26–39, Aug. 2018, doi: 10.1016/j.est.2018.04.020.
- [2] B. Mao, C. Zhao, H. Chen, Q. Wang, and J. Sun, "Experimental and modeling analysis of jet flow and fire dynamics of 18650-type lithium-ion battery," *Appl. Energy*, vol. 281, Jan. 2021, Art. no. 116054, doi: 10.1016/j.apenergy.2020.116054.
- [3] A. Barré, F. Suard, M. Gérard, M. Montaru, and D. Riu, "Statistical analysis for understanding and predicting battery degradations in real-life electric vehicle use," *J. Power Sources*, vol. 245, pp. 846–856, Jan. 2014, doi: 10.1016/j.jpowsour.2013.07.052.
- [4] X. Feng, S. Zheng, D. Ren, X. He, L. Wang, H. Cui, X. Liu, C. Jin, F. Zhang, C. Xu, H. Hsu, S. Gao, T. Chen, Y. Li, T. Wang, H. Wang, M. Li, and M. Ouyang, "Investigating the thermal runaway mechanisms of lithium-ion batteries based on thermal analysis database," *Appl. Energy*, vol. 246, pp. 53–64, Jul. 2019, doi: 10.1016/j.apenergy.2019.04.009.
- [5] G. Zhang, X. Wei, X. Tang, J. Zhu, S. Chen, and H. Dai, "Internal short circuit mechanisms, experimental approaches and detection methods of lithium-ion batteries for electric vehicles: A review," *Renew. Sustain. Energy Rev.*, vol. 141, May 2021, Art. no. 110790, doi: 10.1016/j.rser.2021.110790.
- [6] P. Bangalore and L. B. Tjernberg, "An artificial neural network approach for early fault detection of gearbox bearings," *IEEE Trans. Smart Grid*, vol. 6, no. 2, pp. 980–987, Mar. 2015, doi: 10.1109/TSG.2014.2386305.
- [7] M.-K. Tran and M. Fowler, "A review of lithium-ion battery fault diagnostic algorithms: Current progress and future challenges," *Algorithms*, vol. 13, no. 3, p. 62, Mar. 2020, doi: 10.3390/a13030062.
- [8] Y. Zhang, T. Li, X. Yan, L. Wang, J. Zhang, X. Diao, and B. Li, "Electric vehicle charging fault monitoring and warning method based on battery model," *World Electr. Vehicle J.*, vol. 12, no. 1, p. 14, Jan. 2021, doi: 10.3390/wevj12010014.
- [9] M.-K. Tran, M. Mathew, S. Janhunen, S. Panchal, K. Raahemifar, R. Fraser, and M. Fowler, "A comprehensive equivalent circuit model for lithium-ion batteries, incorporating the effects of state of health, state of charge, and temperature on model parameters," *J. Energy Storage*, vol. 43, Nov. 2021, Art. no. 103252, doi: 10.1016/j.est.2021.103252.
- [10] W. Song, "Research on integrated safety warning and protection system of electric vehicle charging," M.S. thesis, Nanjing Univ. Posts Telecommun., 2019, vol. 2.
- [11] L. Qian, M. Zhao, and W. Zhang, "A method to design the security early warning model of EV charging," *Adv. Power Syst. Hydroelectr. Eng.*, vol. 32, no. 12, pp. 114–119, 2016.
- [12] Y. Zhao, P. Liu, Z. Wang, L. Zhang, and J. Hong, "Fault and defect diagnosis of battery for electric vehicles based on big data analysis methods," *Appl. Energy*, vol. 207, pp. 354–362, Dec. 2017, doi: 10.1016/j.apenergy.2017.05.139.
- [13] L. Zhang, T. Gao, G. Cai, and K. L. Hai, "Research on electric vehicle charging safety warning model based on back propagation neural network optimized by improved gray wolf algorithm," *J. Energy Storage*, vol. 49, May 2022, Art. no. 104092, doi: 10.1016/j.est.2022.104092.
- [14] B. Xia, Y. Shang, T. Nguyen, and C. Mi, "A correlation based fault detection method for short circuits in battery packs," *J. Power Sources*, vol. 337, pp. 1–10, Jan. 2017, doi: 10.1016/j.jpowsour.2016.11.007.
- [15] D. Gao, Y. Wang, X. Zheng, and Q. Yang, "A fault warning method for electric vehicle charging process based on adaptive deep belief network," *World Electr. Vehicle J.*, vol. 12, no. 4, p. 265, Dec. 2021, doi: 10.3390/wevj12040265.

[16] K. Zhang, Z. Yin, X. Yang, Z. Yan, and Y. Huang, "Quantitative assessment of electric safety protection for electric vehicle charging equipment," in *Proc. Int. Conf. Circuits, Devices Syst. (ICCCDS)*, Sep. 2017, pp. 89–94.

[17] Y. Jing, "Research on safety monitoring and fault warning method of electric vehicle charging based on data mining technology," M.S. thesis, North China Electr. Power Univ., vol. 3, 2022, doi: [10.27139/d.cnki.gnbdu.2021.000707](https://doi.org/10.27139/d.cnki.gnbdu.2021.000707).

[18] R. Yang, R. Xiong, S. Ma, and X. Lin, "Characterization of external short circuit faults in electric vehicle Li-ion battery packs and prediction using artificial neural networks," *Appl. Energy*, vol. 260, Feb. 2020, Art. no. 114253, doi: [10.1016/j.apenergy.2019.114253](https://doi.org/10.1016/j.apenergy.2019.114253).

[19] L. Jiang, Z. Deng, X. Tang, L. Hu, X. Lin, and X. Hu, "Data-driven fault diagnosis and thermal runaway warning for battery packs using real-world vehicle data," *Energy*, vol. 234, Nov. 2021, Art. no. 121266, doi: [10.1016/j.energy.2021.121266](https://doi.org/10.1016/j.energy.2021.121266).

[20] J. Lamb, C. J. Orendorff, L. A. M. Steele, and S. W. Spangler, "Failure propagation in multi-cell lithium ion batteries," *J. Power Sources*, vol. 283, pp. 517–523, Jun. 2015, doi: [10.1016/j.jpowsour.2014.10.081](https://doi.org/10.1016/j.jpowsour.2014.10.081).

[21] J. Hou, X. Feng, L. Wang, X. Liu, A. Ohma, L. Lu, D. Ren, W. Huang, Y. Li, M. Yi, Y. Wang, J. Ren, Z. Meng, Z. Chu, G.-L. Xu, K. Amine, X. He, H. Wang, Y. Nitta, and M. Ouyang, "Unlocking the self-supported thermal runaway of high-energy lithium-ion batteries," *Energy Storage Mater.*, vol. 39, pp. 395–402, Aug. 2021, doi: [10.1016/j.ensm.2021.04.035](https://doi.org/10.1016/j.ensm.2021.04.035).

[22] B. Liu, "Design of charging control flow based on electric vehicles," *Automobile Parts*, vol. 147, no. 9, pp. 6–9, 2020, doi: [10.19466/j.cnki.1674-1986.2020.09.002](https://doi.org/10.19466/j.cnki.1674-1986.2020.09.002).

[23] Y. Wu and Y. Wang, "Review of internal short circuit of lithium-ion battery," *Mach. Building Autom.*, vol. 49, no. 4, pp. 169–172, 2020.

[24] D. Ouyang, Y. He, M. Chen, J. Liu, and J. Wang, "Experimental study on the thermal behaviors of lithium-ion batteries under discharge and overcharge conditions," *J. Thermal Anal. Calorimetry*, vol. 132, no. 1, pp. 65–75, Apr. 2018, doi: [10.1007/s10973-017-6888-x](https://doi.org/10.1007/s10973-017-6888-x).

[25] X. Cheng, R. Zhang, C. Zhao, F. Wei, J. Zhang, and Q. Zhang, "A review of solid electrolyte interphases on lithium metal anode," *Adv. Sci.*, vol. 3, no. 3, Mar. 2016, Art. no. 1500213, doi: [10.1002/advs.201500213](https://doi.org/10.1002/advs.201500213).

[26] Y. Liu, C. Zhang, J. Jiang, W. Zhang, and L. Zhang, "Research on capacity difference identification method of lithium-ion battery pack," *Proc. CSEE*, vol. 41, no. 4, pp. 1422–1430, 2021, doi: [10.13334/j.0258-8013.PCSEE.200483](https://doi.org/10.13334/j.0258-8013.PCSEE.200483).



TIAN GAO is pursuing the master's degree with Northeast Electric Power University, Jilin, China. His research interest includes electric vehicle charging safety warning considering multi-factor coupling.



LIANG ZHANG (Member, IEEE) received the M.S. and Ph.D. degrees in electrical engineering and automation from the Harbin Institute of Technology, Harbin, China, in 2010 and 2015, respectively. He is currently an Associate Professor with the Department of Electrical Engineering, Northeast Electric Power University, Jilin, China. His current research interests include cover vehicle-grid coupling, demand side response, and V2G intelligent information interaction.



JUNYU ZHANG is pursuing the master's degree with Northeast Electric Power University, Jilin, China. His research interest includes electric vehicle charging early warning safety.



XIAOHONG DIAO received the M.S. degree from the China Electric Power Research Institute, Beijing, China. Her research interests include electric vehicle charging technology and electric vehicle charging safety warning.



LONGFEI WANG is pursuing the master's degree with Northeast Electric Power University, Jilin, China. His research interest includes energy storage battery fault diagnosis.



LINRU JIANG received the M.S. degree from Nanjing Normal University, Jiangsu, China. Her research interests include electric vehicle charging technology and electric vehicle charging safety warning.



QIZHI WU is pursuing the master's degree with Northeast Electric Power University, Jilin, China. His research interest includes electric vehicle battery charge and discharge warning.

...